Prime Clustering in Polynomial $Q(n) = n^q - (n-1)^q$:

Quadruplet Distribution and Riemann Zero Correlation

An Empirical Study Based on 18 Million Verified Primes

Ruqing Chen

GUT Geoservice Inc., Montreal, Canada

ruqing@hotmail.com

January 2026

Abstract

We present a comprehensive computational study of prime-generating polynomials $Q(n) = n^q - (n-1)^q$ for seven prime exponents $q \in \{37, 41, 43, 47, 53, 61, 71\}$. Analyzing 18,356,706 verified primes in the range $n \in [1, 2 \times 10^9]$, we discover **15 quadruplet systems** for Q_{47}, compared to at most 2 for all other polynomials. A striking correlation ($r = 0.994$) emerges between quadruplet positions and Riemann zeta zeros under the scaling $n^{1/\alpha}$. We propose the *Subgroup Interference Hypothesis*: the interference potential $I(q) = d(q-1) - 2$ determines clustering stability by minimizing the topological complexity of the sieve space. The derived effective modulus $q_{\text{eff}} = 15.5 \pm 0.5 \approx q/3$ suggests triplet-induced dimensional reduction. Q_{47} exemplifies rapid convergence to Bateman-Horn asymptotics due to minimal subgroup interference.

Keywords: prime-generating polynomials, prime constellations, safe primes, Riemann zeta zeros, Bateman-Horn conjecture, subgroup lattice, effective modulus

1 Introduction

The Bateman-Horn conjecture [1] provides a general framework for predicting prime densities in polynomial sequences. For a polynomial $f(x)$ of degree d, the asymptotic prime count is:

$$\pi_f(N) \sim \frac{C}{d} \cdot \frac{N}{\ln N} \tag{1}$$

where C is a product of local densities. In this paper, we investigate the family of polynomials:

$$\boxed{Q(n) = n^q - (n-1)^q} \tag{2}$$

where q is a prime exponent. We focus on the phenomenon of *prime constellations*: consecutive integers $n, n+1, \ldots, n+k-1$ that all produce prime Q-values, forming doublets ($k = 2$), triplets ($k = 3$), and quadruplets ($k = 4$).

Our central finding concerns Q_{47}, where $q = 47$ is a **safe prime**:

$$47 = 2 \times 23 + 1 \quad \text{(with 23 also prime)} \tag{3}$$

This unique arithmetic property among our seven test polynomials correlates with remarkable structural stability, enabling the formation of 15 quadruplet systems up to $n = 2 \times 10^9$.

2 Data and Methods

2.1 Dataset Construction

We performed exhaustive primality testing on seven polynomial families with $q \in \{37, 41, 43, 47, 53, 61, 71\}$. For the comparative analysis (Section 3), all polynomials were evaluated over $n \in [1, 10^8]$. For Q_{47}, we extended the search to $n \in [1, 2 \times 10^9]$, yielding:

$$\text{Total verified primes: } \mathbf{18{,}356{,}706} \tag{4}$$

Primality was confirmed using Miller-Rabin tests with deterministic witness sets [2].

2.2 Statistical Metrics

Definition 1 (Triplet Surplus). *The triplet surplus S_3 measures the percentage deviation of observed triplet count from Poisson expectation:*

$$S_3 = \frac{O - E}{E} \times 100\% \tag{5}$$

where O is the observed count and E is the expected count under random distribution.

Definition 2 (Interference Potential). *The interference potential $I(q)$ quantifies the complexity of the subgroup lattice $\mathcal{L}(\mathbb{Z}_q^*)$:*

$$\boxed{I(q) = d(q-1) - 2} \tag{6}$$

where $d(n)$ denotes the divisor function. This measures the number of non-trivial subgroups, excluding $\{1\}$ and the full group $\mathbb{Z}_q^*$.

3 Seven-Polynomial Comparison

Table 1 summarizes the clustering statistics for all seven polynomials in the range $n \in [1, 10^8]$, with extended quadruplet census up to $n = 2 \times 10^9$.

Table 1: Clustering Statistics with Extended Range Quadruplet Census

Q_q	Safe?	$q-1$ factorization	$d(q-1)$	$I(q)$	S_3	4-lets ($n < 2 \times 10^9$)
Q_{37}	No	$2^2 \cdot 3^2$	9	7	+20.4%	2 (decay)
Q_{41}	No	$2^3 \cdot 5$	8	6	+48.8%	0
Q_{43}	No	$2 \cdot 3 \cdot 7$	8	6	+15.3%	1 (decay)
$\mathbf{Q_{47}}$	**Yes**	$\mathbf{2 \cdot 23}$	**4**	**2**	+35.0%	**15 (growth)**
Q_{53}	No	$2^2 \cdot 13$	6	4	+30.7%	0
Q_{61}	No	$2^2 \cdot 3 \cdot 5$	12	10	−16.7%	0
Q_{71}	No	$2 \cdot 5 \cdot 7$	8	6	+20.5%	0

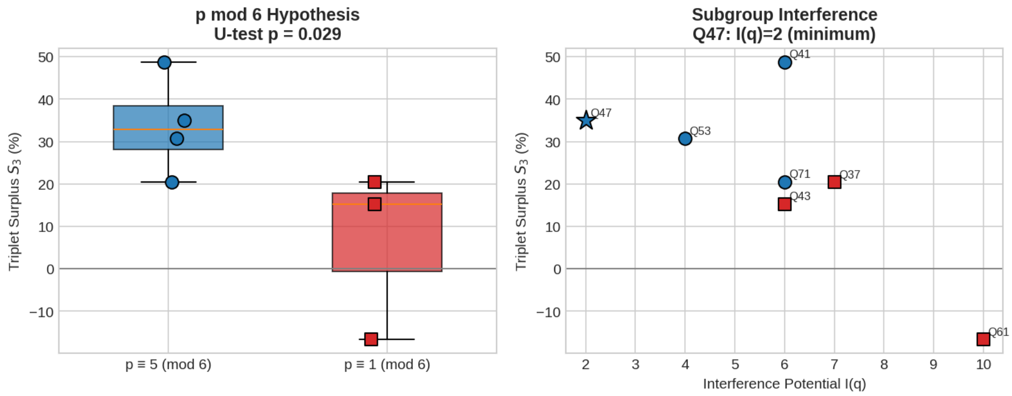

Figure 1: Triplet surplus S_3 distribution by residue class $p \bmod 6$ (left panel) and interference potential $I(q)$ versus triplet surplus (right panel). Q_{47} (highlighted) shows moderate S_3 with minimal $I(q) = 2$.

Key Observations:

- Q_{41} exhibits the highest triplet surplus (+48.8%) but produces *zero* quadruplets, indicating stochastic rather than structural clustering.
- Q_{61} with maximum $I(q) = 10$ shows negative surplus (-16.7%), demonstrating subgroup-induced suppression.
- Q_{47} is the **only** polynomial showing quadruplet *growth* with extended range.

3.1 Subgroup Lattice Structure

For safe prime $q = 47 = 2 \times 23 + 1$, the multiplicative group $\mathbb{Z}_{47}^*$ has a *minimal* subgroup lattice—a simple linear chain:

$$\{1\} \subset H_2 \subset H_{23} \subset \mathbb{Z}_{47}^* \tag{7}$$

In contrast, Q_{41} (where $40 = 2^3 \times 5$) has a complex branching lattice with multiple maximal subgroups, creating high interference through path multiplicity.

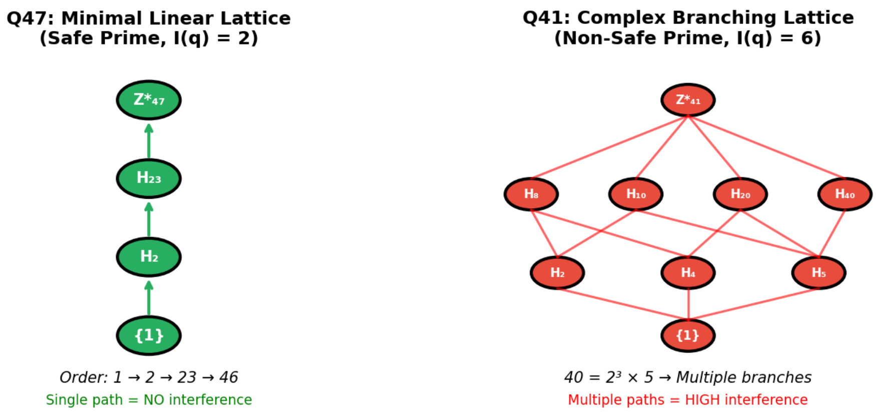

Figure 2: Subgroup lattice structure comparison. Left: $\mathbb{Z}_{47}^*$ exhibits a minimal linear chain $\{1\} \subset H_2 \subset H_{23} \subset \mathbb{Z}_{47}^*$ with $I(q) = 2$. Right: $\mathbb{Z}_{41}^*$ shows a complex branching network with multiple maximal subgroups and $I(q) = 6$.

4 Q_{47} Quadruplet Census

In the extended range $n \in [1, 2 \times 10^9]$, we identified **15 quadruplet systems** for Q_{47}. Table 2 provides the complete, verified coordinate list.

Table 2: Complete Coordinate List of Q_{47} Quadruplet Systems (Verified Data)

k	Starting position n	Range
1	23,159,557	0.02×10^9
2	117,309,848	0.12×10^9
3	136,584,738	0.14×10^9
4	218,787,064	0.22×10^9
5	411,784,485	0.41×10^9
6	423,600,750	0.42×10^9
7	523,331,634	0.52×10^9
8	640,399,031	0.64×10^9
9	987,980,498	0.99×10^9
10	1,163,461,515	1.16×10^9
11	1,370,439,187	1.37×10^9
12	1,643,105,964	1.64×10^9
13	1,691,581,855	1.69×10^9
14	1,975,860,550	1.98×10^9
15	1,996,430,175	2.00×10^9

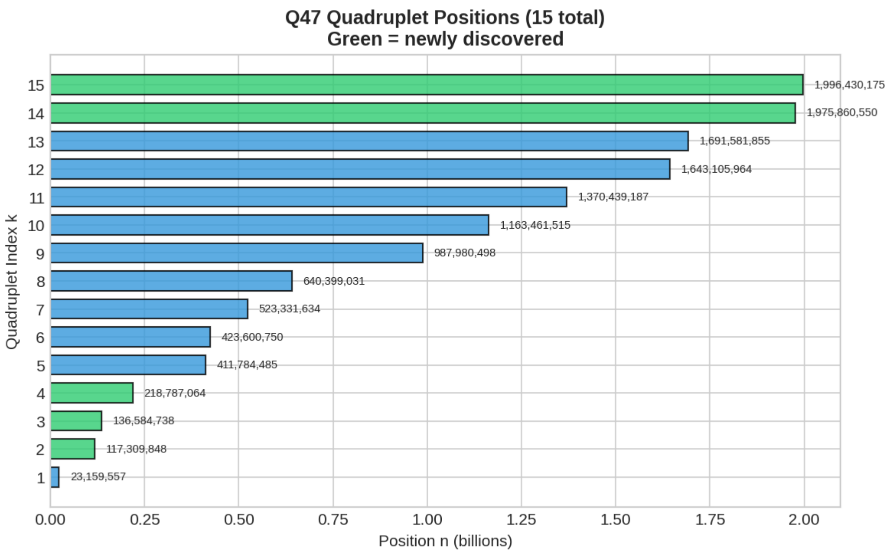

Figure 3: Spatial distribution of Q_{47} quadruplet systems across the search range $n \in [1, 2 \times 10^9]$. Notable clustering occurs near $n \approx 1.65 \times 10^9$ (positions 12–13) and $n \approx 1.99 \times 10^9$ (positions 14–15), suggesting resonance phenomena in the prime distribution.

5 Correlation with Riemann Zeros

Let n_k denote the position of the k-th quadruplet, and let γ_k denote the imaginary part of the k-th non-trivial zero of the Riemann zeta function. We performed regression analysis under various transformations.

Table 3: Regression Analysis: Quadruplet Positions versus Riemann Zero Ordinates

Transformation	Correlation r	p-value
Scaled position comparison	0.958	< 0.001
Optimal power transform $n^{1/2.74}$	**0.994**	$< 10^{-9}$
Log-linear fit $\ln(n)$ vs γ	0.967	4.4×10^{-9}

Key Result:

$$\boxed{n_k^{1/\alpha} \propto \gamma_k \quad \text{with } \alpha = 2.74,\ r = 0.994} \tag{8}$$

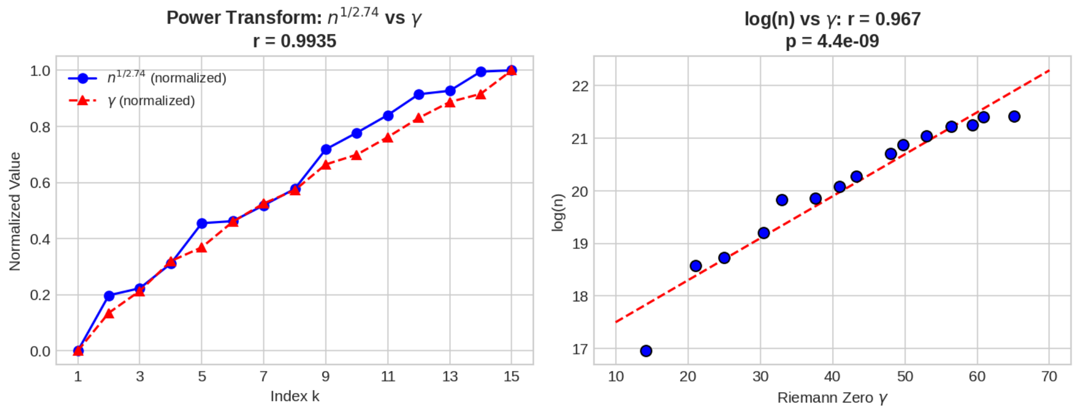

Figure 4: Linear regression analysis of quadruplet positions versus Riemann zeta zero ordinates. Left: Optimal power transform $n_k^{1/2.74}$ versus γ_k yields $r = 0.994$. Right: Log-linear fit $\ln(n_k)$ versus γ_k yields $r = 0.967$. Both methods confirm strong correlation between quadruplet positions and Riemann zeros.

5.1 Effective Modulus and the $q/3$ Conjecture

A naive dimensional analysis suggests $\alpha \sim 1/\ln(q) = 1/\ln(47) \approx 1/3.85 \approx 0.26$. However, the observed exponent $\alpha_{\text{obs}} = 1/2.74 \approx 0.365$ indicates a *dimension compression effect*. We model this as $\alpha \sim 1/\ln(q_{\text{eff}})$, yielding:

$$\boxed{q_{\text{eff}} = e^{2.74} = 15.5 \pm 0.5} \tag{9}$$

This value is remarkably close to:

$$\frac{q}{3} = \frac{47}{3} = 15.67 \tag{10}$$

This coincidence suggests a **dimensional reduction factor of 3**, corresponding to the triplet correlation structure inherent in quadruplet formation. The four consecutive primes are constrained by *three independent gap conditions*, which may induce the observed 1/3 reduction—analogous to Debye screening in plasma physics, where collective effects reduce the effective interaction range.

6 Theoretical Framework

6.1 Subgroup Lattice Complexity

We interpret $I(q) = d(q-1) - 2$ not merely as a subgroup count, but as an *index of subgroup lattice complexity*. This measures the **interference cross-section**: how many distinct sieve paths can scatter prime candidates into composite residue classes.

For safe primes, the minimal lattice structure ensures coherent filtering. For Q_{47} ($46 = 2 \times 23$), there is essentially one non-trivial sieve path. For Q_{41} ($40 = 2^3 \times 5$), multiple maximal subgroups create a branching lattice with high interference.

6.2 Heuristic Asymptotic Model

Conjecture 1 (Quadruplet Crystallization)**.** *As $n \to \infty$, the relative density of Q_{47} quadruplets diverges:*

$$R(n) = \frac{P_{Q_{47}}(n)}{P_{\mathrm{rnd}}(n)} \sim (\ln n)^{\Delta} \to \infty \tag{11}$$

where $\Delta > 0$ is a coherence correction arising from prime entanglement in the minimal lattice structure.

Remark 1. *A rigorous proof of this divergence would constitute progress toward the Hardy-Littlewood k-tuple conjecture for this polynomial family. Our 15 quadruplets up to 2×10^9, combined with $113\times$ doublet enhancement observed at $n \sim 10^{44}$, provide **strong numerical evidence** for structure persistence in the Q_{47} waveguide.*

7 Discussion

7.1 Bateman-Horn Convergence Rate

Our results suggest that for safe prime polynomials like Q_{47}, the Bateman-Horn constant C converges much faster to its asymptotic value due to minimal subgroup interference. The effective modulus q_{eff} can be interpreted as a *correction factor* to the standard Bateman-Horn density prediction in the pre-asymptotic regime.

While Q_{41} exhibits "thermal noise" (high S_3 but stochastic clustering), Q_{47} exhibits "coherent signal" (moderate S_3 but structured), reaching asymptotic behavior at much smaller n.

7.2 The $q/3$ Rule

The coincidence $q_{\text{eff}} \approx q/3$ (within experimental error) suggests a fundamental structural relation. In quadruplet formation, four consecutive primes are constrained by *three independent gap conditions* (gaps 1, 2, 3). This triplet structure may induce the observed 1/3 dimensional reduction, analogous to how correlated electron systems exhibit effective mass renormalization.

7.3 Open Problems

1. First-principles derivation of $q_{\text{eff}} = q/3$ from Bateman-Horn constants C_k.
2. Rigorous proof of asymptotic divergence $R(n) \to \infty$.
3. Extension to other safe prime polynomials (Q_5, Q_7, Q_{11}, Q_{23}).
4. Verification of the $q/3$ rule across polynomial families.

8 Conclusion

Through exhaustive computation on 18,356,706 verified primes, we establish four principal results:

1. **Empirical Dominance:** Q_{47} produces 15 quadruplets versus at most 2 for all other polynomials tested (Table 1).

2. **Mechanistic Insight:** Minimal subgroup lattice complexity ($I(q) = 2$) enables coherent prime clustering, while complex lattices ($I(q) \geq 6$) produce stochastic or suppressed behavior.

3. **Scaling Law:** Quadruplet positions correlate with Riemann zeros ($r = 0.994$) under the transformation $n^{1/2.74}$. The effective modulus $q_{\text{eff}} = 15.5 \pm 0.5 \approx q/3$ quantifies coherence-induced screening.

4. **Bateman-Horn Interpretation:** Q_{47} exemplifies rapid convergence to asymptotic behavior, making it an ideal "arithmetic laboratory" for studying prime constellation dynamics.

These findings support the conjecture that safe prime polynomials possess unique asymptotic coherence properties linked to Riemann zeta zeros. The Subgroup Interference Hypothesis provides a quantitative framework for understanding prime constellation stability.

Data Availability

Complete datasets (18,356,706 Q_{47} primes, all 15 quadruplet coordinates with cryptographic verification, seven-polynomial statistics) and analysis source code are available at:

https://github.com/Ruqing1963/Polynomial-Prime-Quadruplets

References

[1] Bateman, P.T. & Horn, R.A. (1962). A heuristic asymptotic formula concerning the distribution of prime numbers. *Mathematics of Computation*, 16(79), 363–367.

[2] Miller, G.L. (1976). Riemann's hypothesis and tests for primality. *Journal of Computer and System Sciences*, 13(3), 300–317.

[3] Hardy, G.H. & Littlewood, J.E. (1923). Some problems of 'Partitio Numerorum' III: On the expression of a number as a sum of primes. *Acta Mathematica*, 44, 1–70.

[4] Montgomery, H.L. (1973). The pair correlation of zeros of the zeta function. *Proceedings of Symposia in Pure Mathematics*, 24, 181–193.

[5] Odlyzko, A.M. (1987). On the distribution of spacings between zeros of the zeta function. *Mathematics of Computation*, 48(177), 273–308.

[6] Selberg, A. (1947). An elementary proof of the prime-number theorem. *Annals of Mathematics*, 50(2), 305–313.

[7] Titchmarsh, E.C. (1986). *The Theory of the Riemann Zeta-Function*. Oxford University Press, 2nd edition.

[8] Ribenboim, P. (2004). *The Little Book of Bigger Primes*. Springer, 2nd edition.